

## New measurement of the $^{242}\text{Pu}(n,\gamma)$ cross section at n\_TOF

J. Leredegui-Marco<sup>1,a</sup>, C. Guerrero<sup>1</sup>, M. A. Cortés-Giraldo<sup>1</sup>, J. M. Quesada<sup>1</sup>, E. Mendoza<sup>2</sup>, D. Cano-Ott<sup>2</sup>, K. Eberhardt<sup>3</sup>, A. Junghans<sup>4</sup>, and the n\_TOF Collaboration<sup>5</sup>

<sup>1</sup>*Dpto. de Física Atómica, Molecular y Nuclear, Universidad de Sevilla, 41012 Sevilla, Spain*

<sup>2</sup>*Centro de Investigaciones Energéticas, Medioambientales y Tecnológicas (CIEMAT), 28040 Madrid, Spain*

<sup>3</sup>*Johannes Gutenberg-Universität Mainz, 55128 Mainz, Germany*

<sup>4</sup>*Helmholtz-Zentrum Dresden-Rossendorf, D-01314 Dresden, Germany*

<sup>5</sup>*European Center for Nuclear Research (CERN), CH-1211 Geneva, Switzerland*

**Abstract.** The use of MOX fuel (mixed-oxide fuel made of  $\text{UO}_2$  and  $\text{PuO}_2$ ) in nuclear reactors allows substituting a large fraction of the enriched Uranium by Plutonium reprocessed from spent fuel. With the use of such new fuel composition rich in Pu, a better knowledge of the capture and fission cross sections of the Pu isotopes becomes very important. In particular, a new series of cross section evaluations have been recently carried out jointly by the European (JEFF) and United States (ENDF) nuclear data agencies. For the case of  $^{242}\text{Pu}$ , the two only neutron capture time-of-flight measurements available, from 1973 and 1976, are not consistent with each other, which calls for a new time-of-flight capture cross section measurement. In order to contribute to a new evaluation, we have performed a neutron capture cross section measurement at the n\_TOF-EAR1 facility at CERN using four  $\text{C}_6\text{D}_6$  detectors, using a high purity target of 95 mg. The preliminary results assessing the quality and limitations (background, statistics and  $\gamma$ -flash effects) of this new experimental data are presented and discussed, taking into account that the aimed accuracy of the measurement ranges between 7% and 12% depending on the neutron energy region.

### 1 Introduction and motivation

The measurement of accurate capture and fission cross sections is essential for the design and operation of current and innovative nuclear systems aimed at the reduction of the nuclear waste [1]. The spent fuel from current nuclear reactors contains a significant fraction of plutonium, which can be separated from the fuel matrix. This plutonium contains 66% of the fissile  $^{239}\text{Pu}$  and  $^{241}\text{Pu}$ , that can be combined with depleted uranium ( $^{238}\text{U}$ ) to make what is known as mixed oxide (MOX) fuel. In this way the Pu from spent fuel and the depleted uranium, otherwise considered as waste, are used in a new reactor cycle, contributing in this way to the long-term sustainability of nuclear energy. Currently, the use of MOX fuel in thermal power reactors has been established in several countries. However, a much more efficient use of plutonium will ultimately be made in fast reactors, where multiple recycling is possible and has been demonstrated. The reader is referred to Ref.[2] for more details on the status and progress in MOX fuel technologies.

---

<sup>a</sup>e-mail: jleredegui@us.es

**Table 1.** Current and required accuracy for the capture cross section of  $^{242}\text{Pu}$  for different nuclear reactor concepts, including as well the neutron energy range of interest. See Refs. [7, 8]

System	Neutron energy range	Present accuracy (%)	Required accuracy (%)
SFR	2-500 keV	35	8
EFR	2-67 keV	35	25
GFR	2-183 keV	35	7-8
LFR	9-183 keV	35	11-12
ADMAB (ADS)	9-25 keV	35	10
PHENIX	0.5-2 keV	14	7
NEA/HPRL	0.5-2 keV	14	8

The extensive use of MOX fuels in fast reactors calls for a revision of the neutron cross sections that play a role in the neutronics of such reactors and are not known with enough accuracy yet. For the particular case of  $^{242}\text{Pu}$ , the first attempts to measure its neutron capture cross section were made in 1973 and 1976, when Portmans et al. [3] and Hockenbury et al. [4] used the time-of-flight technique for measurements at low (below 1.3 keV) and high (6-87 keV) neutron energies, respectively. A few years later, Wisshak and Kaeppler [5, 6] measured the capture cross section in the 10-90 and 50-250 keV energy intervals. The comparison of the different results indicates an uncertainty of about 35% in the capture cross section in the keV region. In this context, the Nuclear Energy Agency recommends in its “High Priority Request List” [7] and its report WPEC-26 [8] that the capture cross section of  $^{242}\text{Pu}$  should be measured with an accuracy of at least 7-12% in the neutron energy range between 500 eV and 500 keV (see Table 1). Furthermore, interpretations with JEFF-3.1 of the PROFIL and PROFIL-2 experiments carried out in the fast reactor PHENIX have shown an overestimation of about 14% of the  $^{242}\text{Pu}$  capture cross section [9, 10]. In addition to the direct measurement in the fast energy region ( $E_n > 2$  keV), accurate average radiation width and strength function are required to solve some ambiguous results obtained between optical model calculations and the statistical analysis of the s-wave resonance parameters [11]. This calls as well for an accurate measurement of the resonance region (1 to 1000 eV) with enough resolution and statistics to determine accurately the corresponding average resonance parameters.

For all of the above, a new measurement of the  $^{242}\text{Pu}$  cross section at the n\_TOF facility was proposed to the ISOLDE and Neutron Time-of-Flight Committee (INTC) [12] and was approved in September 2013. The material production and sample preparation took place during the first semester of 2015 in collaboration with the JGU Mainz and the HZ Dresden-Rossendorf research centers. Finally, the experiment was successfully performed in summer 2015. In the following section we briefly describe the n\_TOF facility and the experimental setup. Section 3 provides some details on the measuring technique and the preliminary data and some preliminary results are presented in Section 4.

## 2 Experimental setup

The measurement was performed at the n\_TOF-EAR1 facility at CERN [13]. The pulsed neutron beam at n\_TOF is generated through spallation of 20 GeV/c protons from the CERN Proton Synchrotron (CPS) impinging on a thick lead target. Each proton bunch contains, in average,  $7 \cdot 10^{12}$  protons with a time distribution of  $\sigma = 7$  ns and an average repetition rate of 0.17 Hz. The spallation neutrons, with energies in the MeV-GeV range, are partially moderated in the water cooling and moderation layers that surround the lead target and travel towards the experimental areas along two beam lines: EAR1 at 185 m (horizontal) and EAR2 at 19 m (vertical). A complete description and experimental

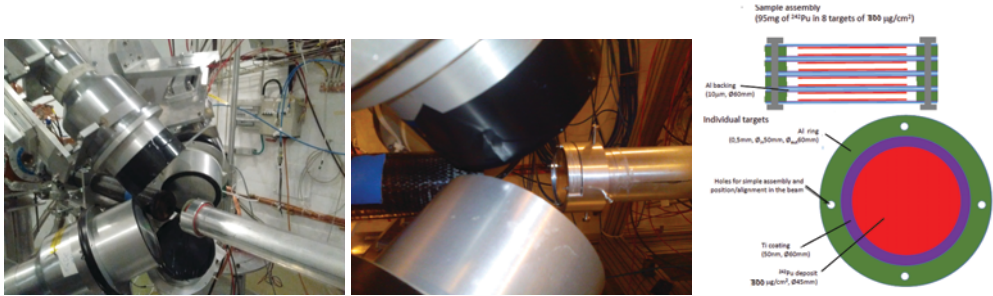


**Figure 1.** Experimental setup for the detection of  $\gamma$ -rays from capture on  $^{242}\text{Pu}$ : (Left) 4  $\text{C}_6\text{D}_6$  detectors looking at the  $^{242}\text{Pu}$  sample assembly (center), composed of by several thin targets (right).

characterization of EAR1 can be found in Ref. [13], while the description of the EAR2 beam line, still in its commissioning phase, is given in Ref. [14]. The measurement presented in this work was performed in EAR1, featuring a better time resolution and consequently a better capability to resolve resonances up to higher neutron energies than in EAR2.

At n\_TOF, the radiative capture measurements can be performed using two different detection systems available: the Total Absorption Calorimeter TAC [15] (a  $4\pi$   $\text{BaF}_2$  array) and the Total Energy detectors (deuterized benzene ( $\text{C}_6\text{D}_6$ ) scintillators [16]). The latter have been chosen for this measurement mainly because they suffer significantly less from the so-called  $\gamma$ -flash, thus allowing us to measure up to the required neutron energy (see Table 1). In addition, this detection setup features a much lower neutron sensitivity than the TAC. This advantage is counterbalanced by a more complicated analysis technique, discussed in Section 3.

Neutrons coming from the spallation target, travel 185 m in vacuum along the beam line until they reach the  $^{242}\text{Pu}$  sample, with a diameter larger than the beam, inducing radiative capture reactions. The  $\gamma$ -ray cascades are detected with 4 *BICRON*  $\text{C}_6\text{D}_6$  scintillators placed at  $\sim 10$  cm of the sample (Figure 1). The gain of the  $\text{C}_6\text{D}_6$  detectors was adjusted to record signals up to 14 MeV in the flash-ADC cards. The detectors were calibrated in energy using five  $\gamma$ -ray energies from  $^{137}\text{Cs}$ ,  $^{88}\text{Y}$ ,  $^{241}\text{Am}$ ,  $^9\text{Be}$  and  $^{244}\text{Cm}$ - $^{13}\text{C}$  and the energy calibration was validated with the comparison between experiment and Geant4 simulations of the detector response to this sources. Upstream from the sample, the neutron beam is monitored with the SiMon monitor which consists of four silicon detectors looking at a thin lithium foil for detecting  $^6\text{Li}(n,\alpha)$  reactions [17]. The signals registered in each detector are recorded by our digital data acquisition system. The new 12-bit cards with a maximum sampling rate of 900MSamples/s enhance the amplitude (deposited energy) resolution, timing and signal reconstruction capabilities.

The sample preparation was carried out within the CHANDA project [18] by the University of Mainz and the HZDR research center. A total of 95 mg of 99% pure  $^{242}\text{Pu}$ , a series of eight thin  $^{242}\text{Pu}$  samples 45mm in diameter were prepared by electrodeposition of  $^{242}\text{Pu}$  on a thin ( $10\ \mu\text{m}$ ) Al backing covered with 50 nm Ti coating, reaching a maximum density of  $0.8\ \text{mg}/\text{cm}^2$  of  $^{242}\text{Pu}$  per sample. The thickness of the backings was minimized to a level where the associated background becomes negligible. The right panel of Figure 1 shows schematic view of the structure of each thin target and the final assembly as a stack of targets.

### 3 Total Energy Detection Technique

Neutron capture measurements with  $C_6D_6$  detectors are analyzed following the *Total Energy Detection Technique* [19, 20], based in two principles. First, the efficiency of the detectors is low enough so that just one  $\gamma$ -ray per cascade is detected and thus the total efficiency to detect a cascade becomes  $\epsilon_c = 1 - \prod_i (1 - \epsilon_i) \approx \sum_i \epsilon_i$ , being  $\epsilon_i$  the efficiency to detect a single gamma of energy  $E_i$ . Second, the efficiency to detect one  $\gamma$ -ray is proportional to its energy. Under these conditions the efficiency for detecting a cascade will be proportional to the known cascade energy ( $E_c$ ) and independent of the actual cascade path:  $\epsilon_c = k \sum_i E_i = k \cdot E_c$ . However, the second condition is not true and needs from mathematical manipulation of the detector response. The measured counts for each deposited energy must be weighted with an energy (pulse height) dependent weighting function (WF); this is known as the *Pulse Height Weighting Technique (PHWT)*.

To calculate the WF, the response distribution of each detector must be well known. Since its experimental determination is impossible due to the lack of monoenergetic  $\gamma$ -ray sources in the whole energy range of interest (0-12 MeV), Monte Carlo simulations, performed in this work using the *Geant4* toolkit [21], are the best solution. In these simulations the details on the experimental setup and the 8-target sample were implemented in order to consider, among other effects, the attenuation of photons in the  $^{242}\text{Pu}$  targets. From these accurate simulations we extract response functions for each detector to a large number of  $\gamma$ -ray energies,  $R_{ij} = \frac{\text{counts}_{ij}}{N_i}$ , where  $j$  represents the bin number for a certain deposited energy and  $i$  is the  $\gamma$ -ray energy. The response functions are appropriately broaden to consider the detectors' energy resolution before being used as the input to obtain the WF. The energy dependence of this resolution is extracted from the fit of the experimental broadenings with simulated responses to calibration sources at different  $\gamma$ -ray energies. The WF's are assumed to be 4<sup>th</sup>-8<sup>th</sup>-degree polynomials,  $W_j = \sum_k a_k \cdot (E_j)^k$ , and their parameters,  $a_k$ , are obtained with the *Minuit* function minimization code. The obtained WF's satisfy (within 2%), in the whole energy range from 100 keV-10 MeV, the proportionality condition

$$\sum_j W_j \cdot R_{ij} = E_i ; \text{ where } \sum_j R_{ij} = \epsilon_i.$$

### 4 Preliminary analysis and first results

The digitalized movies, in the so-called raw data format, are transferred and stored in the CERN Advanced STORage manager (*CASTOR*). This raw data files are processed with a dedicated pulse shape analysis routine [22]. It has been extensively validated to ensure the correct reconstruction of the amplitude, area, time, and all other relevant features of each recorded signal. The output of this program provides files in *ROOT* format, including the correlation of the complete set of variables that characterize the signals. Last, the data reduction is performed with the *TTOFsort* routine (developed by F. Gusing), that implements the energy calibration of the detectors, applies the weighting functions and performs a coincidence rejection to satisfy the condition of detecting just one  $\gamma$ -ray, among many other options. This program provides histograms of detected counts as a function of the time-of-flight, deposited energy, etc...

The measured counts as a function of the time-of-flight (TOF) must then be converted into equivalent neutron energy ( $E_n$ ). Provided that we are in the non-relativistic regime, the relation between these two quantities is given by  $E_n(\text{eV}) = (72.29 \frac{L(m)}{TOF(\mu\text{s})})^2$ , where  $L$  is the flightpath (185m for EAR1). The left panel of Figure 2 shows the counting rates for the  $^{242}\text{Pu}$  sample and the different background contributions, as a function of the neutron energy, between thermal and the aimed 500 keV, normalized to the average pulse intensity of  $7 \cdot 10^{12}$  protons. The so-called *dummy* sample is a replica of the

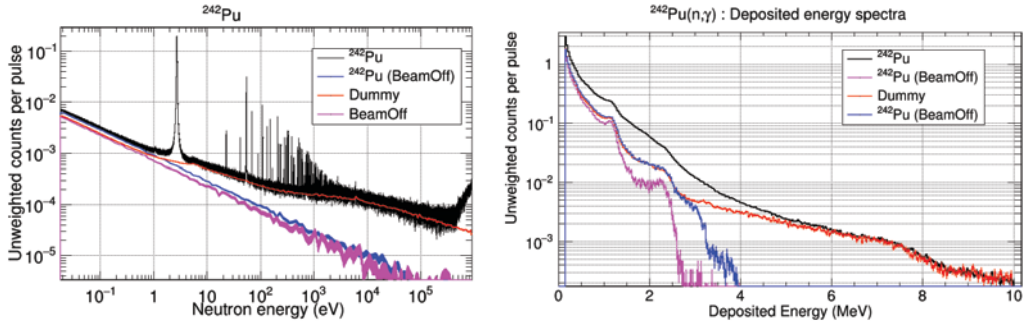


**Figure 2.** Left: Sketch of the individual targets and the assembled stack with 8 targets. Right: Picture of the  $^{242}\text{Pu}$  sample assembly.

$^{242}\text{Pu}$  assembly without  $^{242}\text{Pu}$  deposits inside and is the main neutron related background component. In addition to the contribution of the backings in the sample, we also have to consider the room backgrounds, with and without the  $^{242}\text{Pu}$  targets in place. The ratio of signals from capture on  $^{242}\text{Pu}$  to background can be enhanced with an adequate choice of the conditions in amplitude (or deposited energy  $E_{dep}$ ). The corresponding deposited energy distributions are presented in the right panel of Figure 2, where the preliminary thresholds in  $E_{dep}$  have been set to 150 keV and 10 MeV. This figure shows that the excess of counts coming from  $^{242}\text{Pu}$  are below the neutron separation energy of the compound nucleus,  $S_n=5.035$  MeV. The increase of the beamoff background when the  $^{242}\text{Pu}$  is in place, is thought to come from the spontaneous fission  $\gamma$ -rays.

In order to extract the neutron capture yield,  $Y_{exp}$ , the different background contributions shown in Figure 2 are subtracted from the total counts following a two step process. First the beamoff contributions are subtracted:  $A = {}^{242}\text{Pu} - {}^{242}\text{Pu}_{beamoff}$  and  $B = \text{Dummy} - \text{Beamoff}$ . Then  $C = A - B$ , represents the counts coming from reactions on  $^{242}\text{Pu}$ . However, not every reaction on  $^{242}\text{Pu}$  is induced by neutrons. Indeed, for targets with a high atomic number  $Z$ , an additional background contribution comes from in-beam  $\gamma$ -rays induced reactions (compton  $\propto Z^2$  and pair production  $\propto Z$ ). A high  $Z$  material with negligible neutron capture cross section,  ${}^{nat}\text{Pb}$  in our case, was measured to estimate the level of the in-beam  $\gamma$ -ray induced background, assuming that the  $\gamma$ -ray induced background,  $B_\gamma$ , dependence on  $Z$  and  $n(\text{atoms/barn})$  is given by  $B_\gamma \propto Z^{3/2} \cdot n$ . After scaling the counts in Pb to the expected background in our measurement, the  $\gamma$ -ray background is found to be negligible at low energies and as high as 35% of  $^{242}\text{Pu}$  after subtracting the *dummy* in the hundreds of keV region. In this energy range the reduction of uncertainties will be mainly limited by the systematic uncertainties related to the dummy sample since it represents up to 80% of the total counts.

According to PHWT (see Section 3), from the weighted counts after background subtraction,  $C_w$ , we extract the experimental capture yield as

$$Y_{exp}(E_n) = f_c \cdot f_{sat} \cdot \frac{C_w(E_n)}{\Phi(E_n) \cdot BIF \cdot (S_n + E_n)}$$

where  $\Phi$  represents the accurately measured neutron flux of n\_TOF-EAR1 [23],  $BIF$  stands for Beam Interception Fraction, being the unity since the sample covers the full beam;  $f_c$  is a factor that corrects for the counts lost below the amplitude threshold, the multiple detection of photons and the presence of conversion electrons; and  $f_{norm} = \frac{1}{Y_{sat}}$ , is the normalization factor obtained from the measured saturated value of the capture yield of  ${}^{197}\text{Au}$  at  $E_n = 4.9\text{eV}$ ,  $Y_{sat}$ . In Figure 3, we show

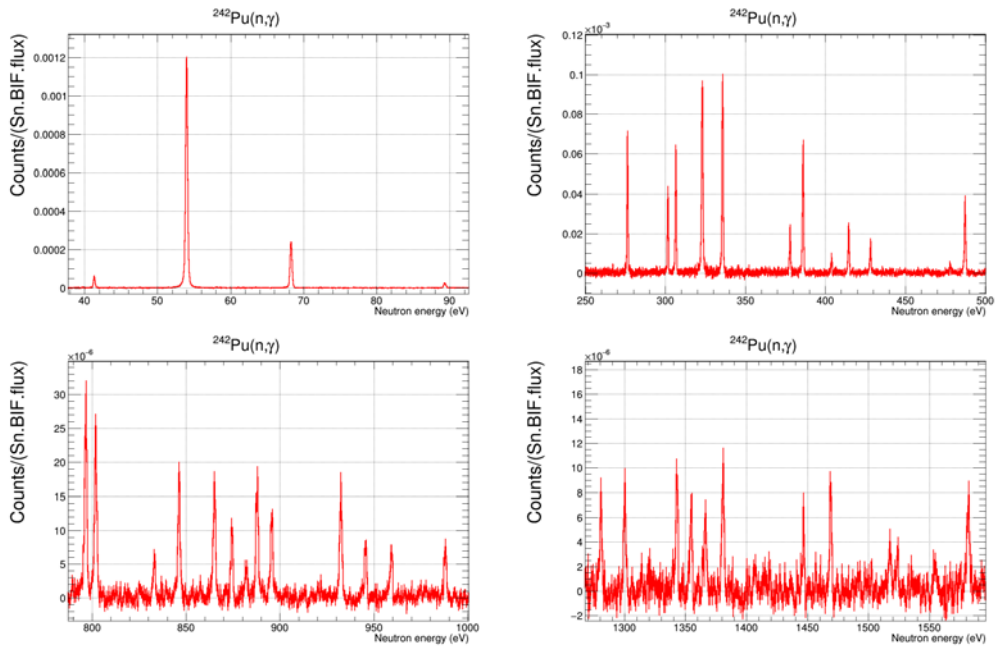


**Figure 3.** Capture counts per incident neutron (not in Yield units) obtained in the RRR from the tenths of eV to  $\sim 1.5$ keV

the preliminary results obtained after dividing the capture counts by the neutron flux, the BIF and  $S_n$ , and thus proportional to the capture yield. Four different energy ranges are shown to illustrate first the high level of statistics in the RRR below 1 keV and the promising results above this energy that hopefully will allow a resonance analysis up to 2keV. Beyond 2 keV we cannot clearly resolve every resonance due to the increasing level density and the limited statistics and we will thus employ the Unresolved Resonance Region (URR) formalism. The capability to extract a reliable cross section in the URR up to 500 keV with this experimental technique and background conditions will be validated with a careful analysis of the  $^{197}\text{Au}(n,\gamma)$  measurement, which presents a standard cross section above 150 keV.

## 5 Summary and conclusions

The use of MOX fuels in innovative nuclear systems requires a better knowledge of the neutron radiative capture cross section on  $^{242}\text{Pu}$ . Following the demands of the Nuclear Energy Agency the new measurement aims to reduce the current uncertainties in the 0.5 to 500 keV region down to 7-12% depending on the energy range. Furthermore, the new experimental data in the RRR, up to at least 1 keV, will allow to reduce the current 10% deviations in the average resonance parameters between the different libraries. The measurement has successfully taken place at n\_TOF-EAR1, that features a very high energy resolution, using 95 mg of 99% pure  $^{242}\text{Pu}$  electrodeposited on 8 thin targets assembled together and covering the full neutron beam. The first results after the preliminary quality checks and background subtraction are promising and we expect to fulfill the proposed goals. A final capture yield will be ready soon and will be followed by a resonance analysis. In the last stage, we

aim to collaborate with the evaluators in CEA Cadarache (JEFF) or ORNL (ENDF) in order to include the new experimental data in the upcoming release of the  $^{242}\text{Pu}(n,\gamma)$  cross section evaluation.

## Acknowledgments

This measurement has received funding from the EC FP7 Programme under the projects NEUTAN-DALUS (Grant No. 334315) and CHANDA (Grant No. 605203), and the Spanish Ministry of Economy and Competitiveness projects FPA2013-45083-P and FPA2014-53290-C2-2-P.

## References

- [1] N. Colonna et al, *Energy Environ. Sci.* **3**, 1910-1917(2010)
- [2] *International Atomic Energy Agency, Status and advances in Mox fuel technology* IAEA Technical Reports Series **415** (2003)
- [3] F. Poortmans et al., *Nucl. Phys A* **207**, 342-352(1973)
- [4] R.W.Hockenbury et al., *SP* **425**, 584-586 (1975)
- [5] K. Wisshak and F. Kaeppler, *Nucl. Sc. and Eng.* **66**, 363 (1978)
- [6] K. Wisshak and F. Kaeppler, *Nucl. Sc. and Eng.* **69**, 39 (1979)
- [7] *NEA High Request Priority List* <http://www.nea.fr/dbdata/hprl/>
- [8] Salvatores and R. Jacqmin, *Uncertainty and target accuracy assessment for innovative system using recent covariance data evaluations* (NEA/WPEC-26, 2008)
- [9] G. Noguere, E. Dupont, J. Tommasi and D. Bernard. Technical note CEA Cadarache, NT-SPRC/LEPH-05/204 (2005)
- [10] J. Tommasi, E. Dupont and P. Marimbeau., *Nucl. Sci. Eng.* **154**, 119-133 (2006)
- [11] E. Rich, G. Noguere, C. De Saint Jean and O. Serot. Proceedings of the Int. Conf. on Nuclear Data for Science and Technology, Nice, France, 2007
- [12] C. Guerrero, E. Mendoza et al. *Radiative capture on  $^{242}\text{Pu}$  for MOX fuel reactors*, CERN-INTC-2013-027 (INTC-P-387) (2013)
- [13] C. Guerrero et al., *Eur. Phys. J. A* **49**, 27(2013)
- [14] C. Weiss et al., *Nucl Instrum. and Meth. A* **799**, 90–98 (2015)
- [15] C.Guerrero et al., *Nucl. Instrum. Methods A* **608**, 424 (2009)
- [16] P. Mastinu et al., *New C6D6 detectors: reduced neutron sensitivity and improved safety*, CERN-n\_TOF-PUB-2013-002 (2013)
- [17] S. Marrone et al., *Nucl. Instrum. Methods A* **517**, 389 (2004).
- [18] *CHANDA:solving CHallenges in Nuclear DAta*. Project funded by FP7-EURATOM-FISSION, European Commission.
- [19] R.L. Macklin, J.H. Gibbons, *Phys. Rev.* **159**, 1007 (1967)
- [20] Abondano et al., *Nucl. Instrum. and Meth. A* **521**, 454–467(2004)
- [21] S. Agostinelli et al., *Nucl. Instrum. Methods A* **506**, 250 (2003)
- [22] P. Zugec et al., *Pulse Shape Analysis routines for n\_TOF-Phase3*. *Nucl. Instrum. Methods A*. To be published (2015)
- [23] M. Barbagallo et al., (The n\_TOF Collaboration), *EPJ A* **49**, 156 (2013)